

# Model supported determination of the process window for aluminothermic synthesis of refractory high entropy alloys

Carolyn Maier<sup>[1]</sup>, Bernd Friedrich<sup>[1]</sup>

[1] IME Process Metallurgy and Metal Recycling - RWTH Aachen University

## Motivation and concept

### Refractory high entropy alloys (RHEA)

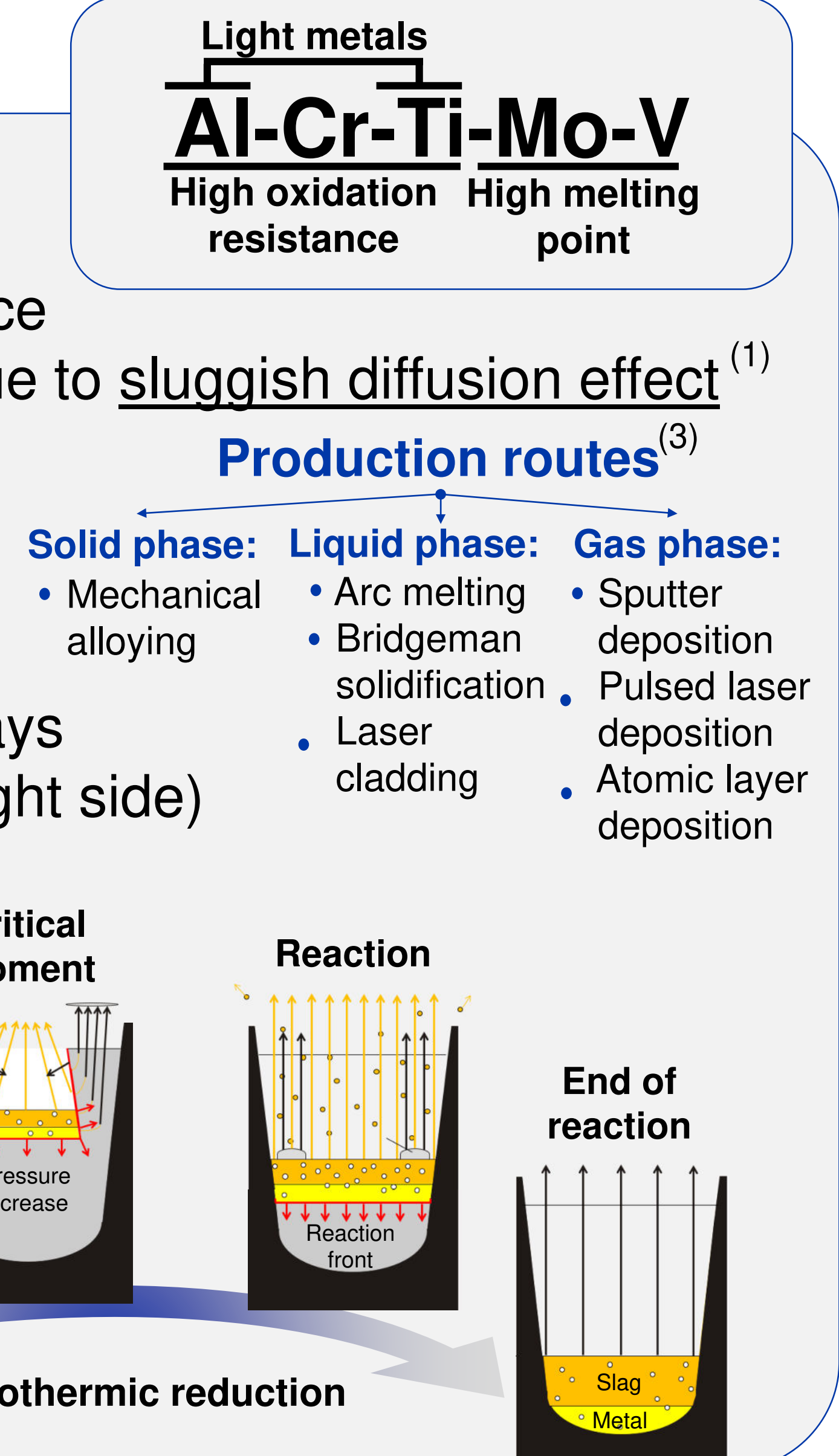
High entropy alloys (HEA) are a young material group of alloys with outstanding properties:

- High strength and hardness through lattice distortion effect and cocktail effect, high corrosion resistance (e.g. compared to stainless steel) through simplified crystal structure and excellent thermal stability due to sluggish diffusion effect<sup>(1)</sup>
- Criteria for HEA<sup>(2)</sup>
  - Number of principal elements  $\geq 5$  with content of each component between 5 and 35 at.-%
  - Maximum of configuration entropy for solution phase
- RHEA contains high-melting refractory metals; the application of these metals can especially improve properties in the high-temperature range and can replace Ni-based superalloys used nowadays
- Most common production process is arc melting; there are a variety of manufacturing methods (see right side)

### Aluminothermic reduction process

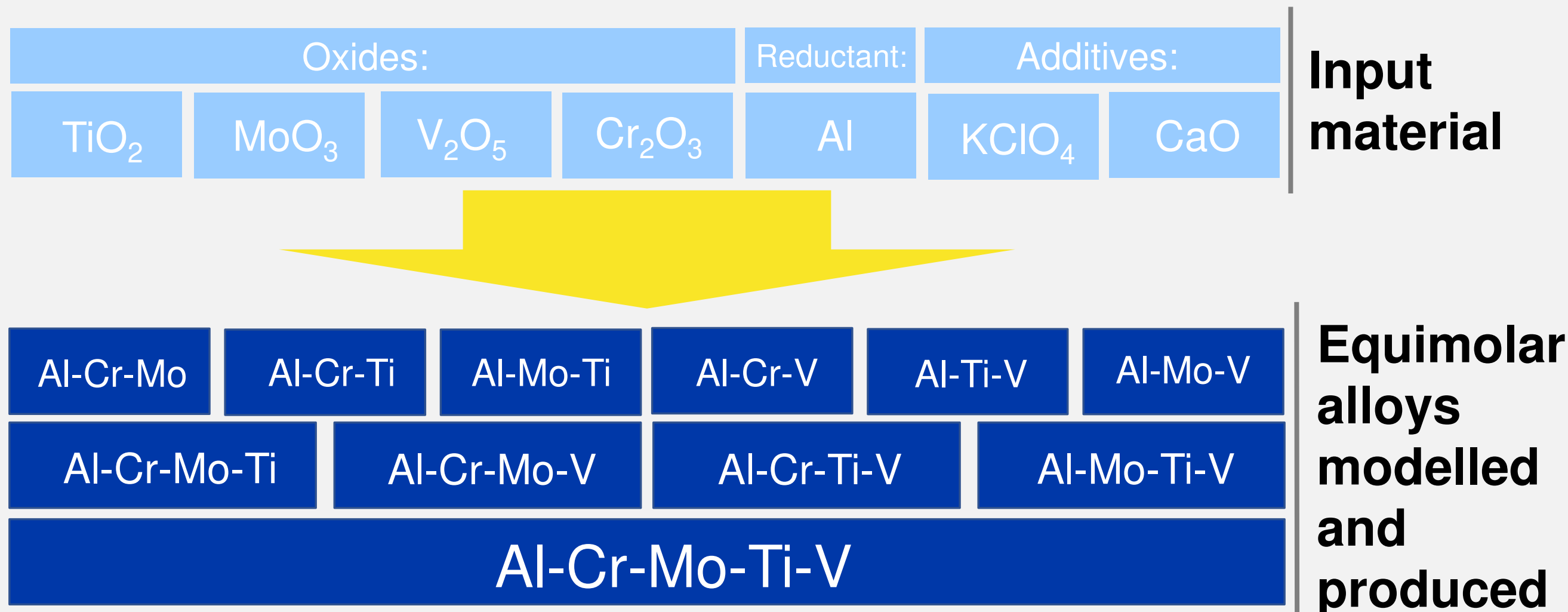
Due to high material and production costs alternative production processes are highly demanded:

- Aluminothermic reduction offers generally a robust and economical process through
  - High temperatures
  - Short reaction times
  - Self-propagating reaction behavior
  - Metal oxide prices lower than metal prices with required purities
- Direct alloy synthesis through co-reduction of all alloying element oxides
  - Exploitation of various thermal energy releases during reduction of different metal oxides



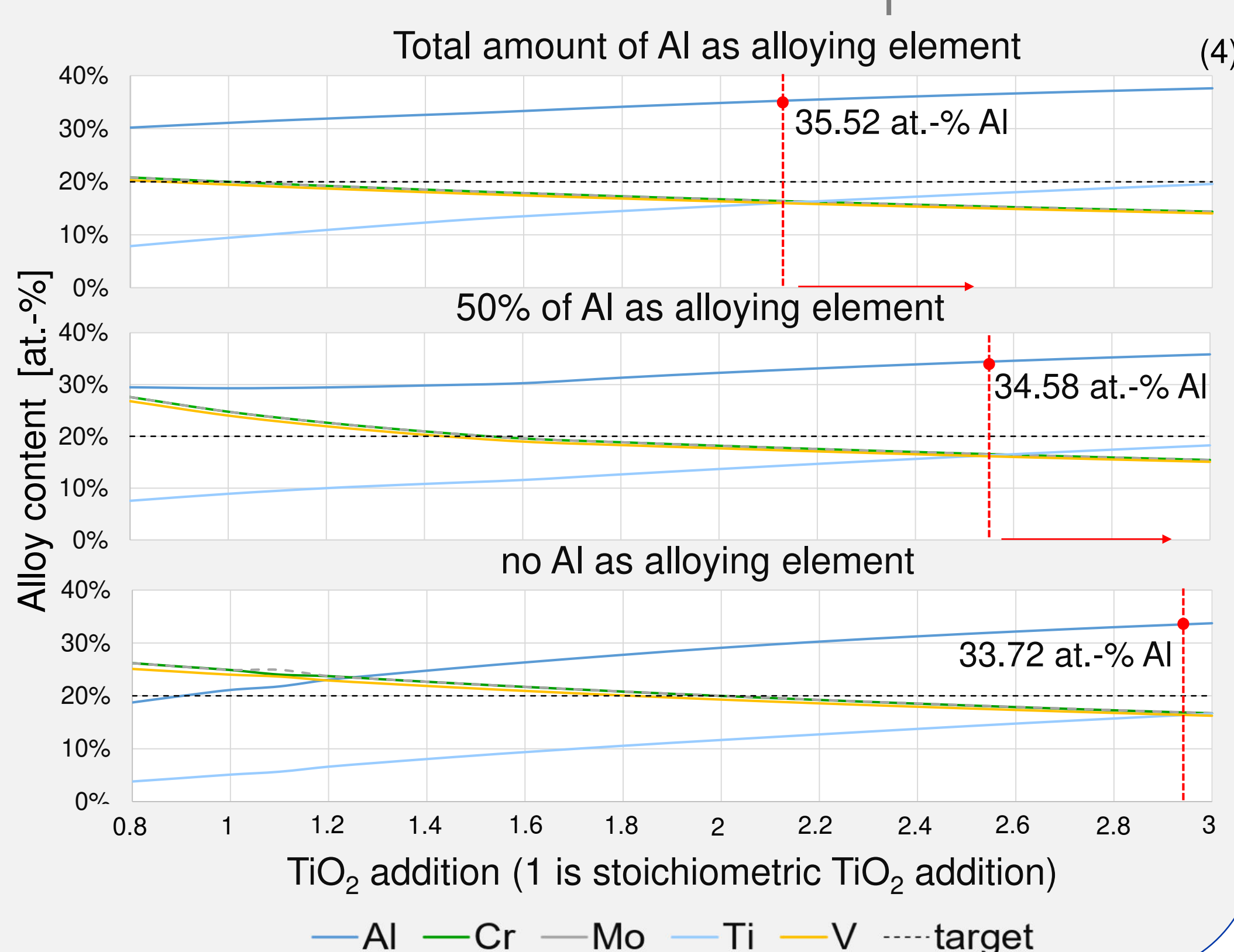
## Thermochemical modelling

- Consideration of different alloys, optimization with regard to optimal composition of the alloy AlCrMoTiV
- Software used: FactSage 8.0; databases used: FactPS, SGTEb, Ftoxid



### Variation of Al mass input

- Higher Al additions lead to equimolar composition of Cr, Mo, Ti and V with lower additions of TiO<sub>2</sub>
- Al content decreases with lower Al addition to input mixture



## Experimental procedure

- Target alloy mass 5000 g, energy density per gram input mixture set to -3000 kJ/g; equimolar composition of metal phase; one repetition
- Intensive investigation of the alloy AlCrMoTiV with variation of the parameters TiO<sub>2</sub> and Al/TiO<sub>2</sub> addition to the mixture
- Metal analysis via ICP-OES, slag analysis via XRF (WROXI)

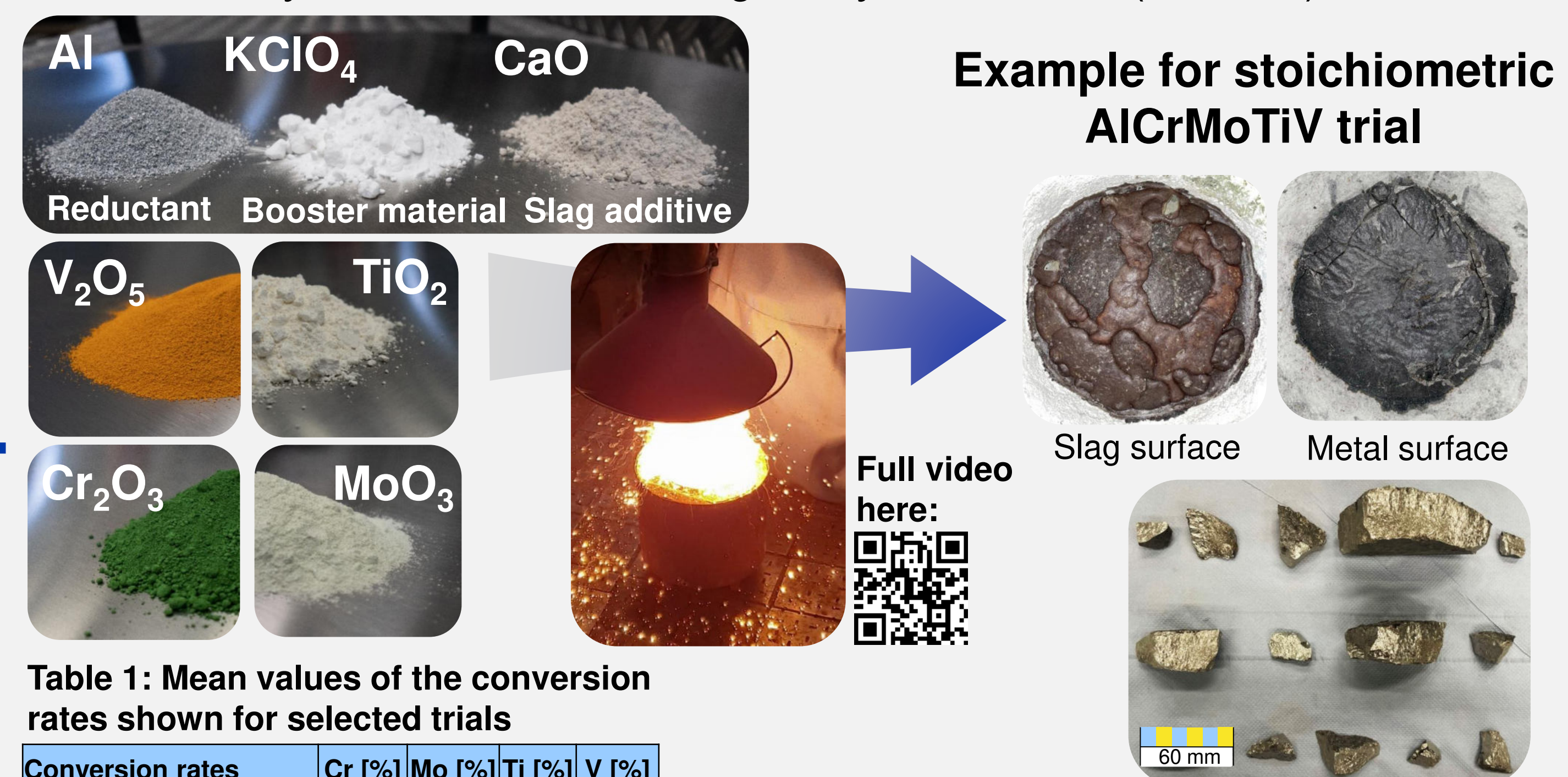
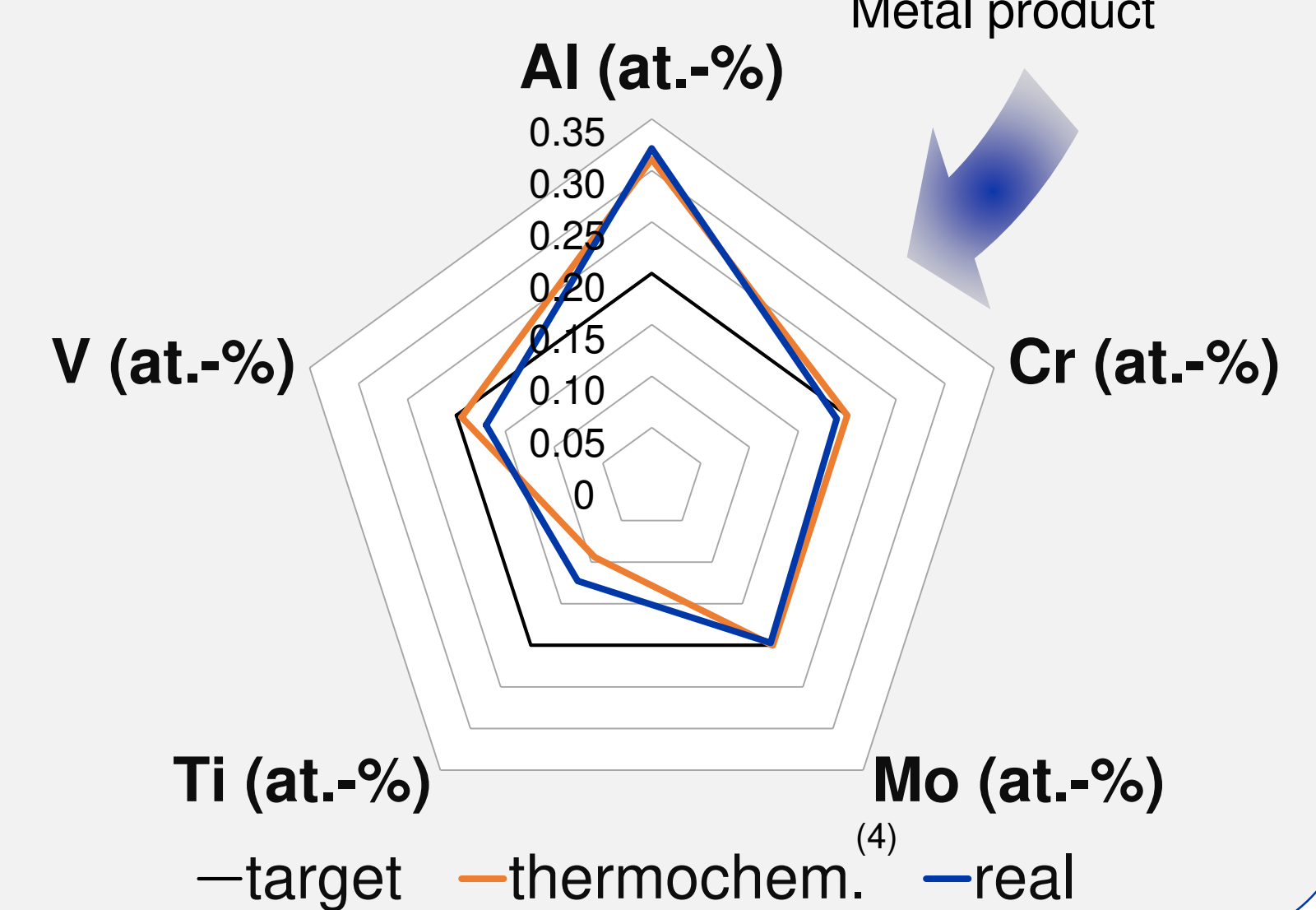


Table 1: Mean values of the conversion rates shown for selected trials

Conversion rates	Cr [%]	Mo [%]	Ti [%]	V [%]
AlCrMo*	83.7	89.1		
AlCrTi*	69.3		44.2	
AlCrV*	89.7			82.1
AlMoTi*		87.8	58.6	
AlMoV*		95.3		84.7
AlTiV*			70.1	92.6
AlCrMoTi*	81.1	89.5	58.7	
AlCrMoV*	86.0	91.3		83.0
AlCrTiV*	92.8		70.4	89.6
AlMoTiV*		87.1	51.8	77.3
AlCrMoTiV*	82.2	90.4	51.2	72.6
AlCrMoTiV (more TiO <sub>2</sub> )	88.1	91.2	69.8	81.5

\*trials were carried out with stoichiometric mixture of oxides and reducing agent



## Assessment

### Aluminothermic RHEA production

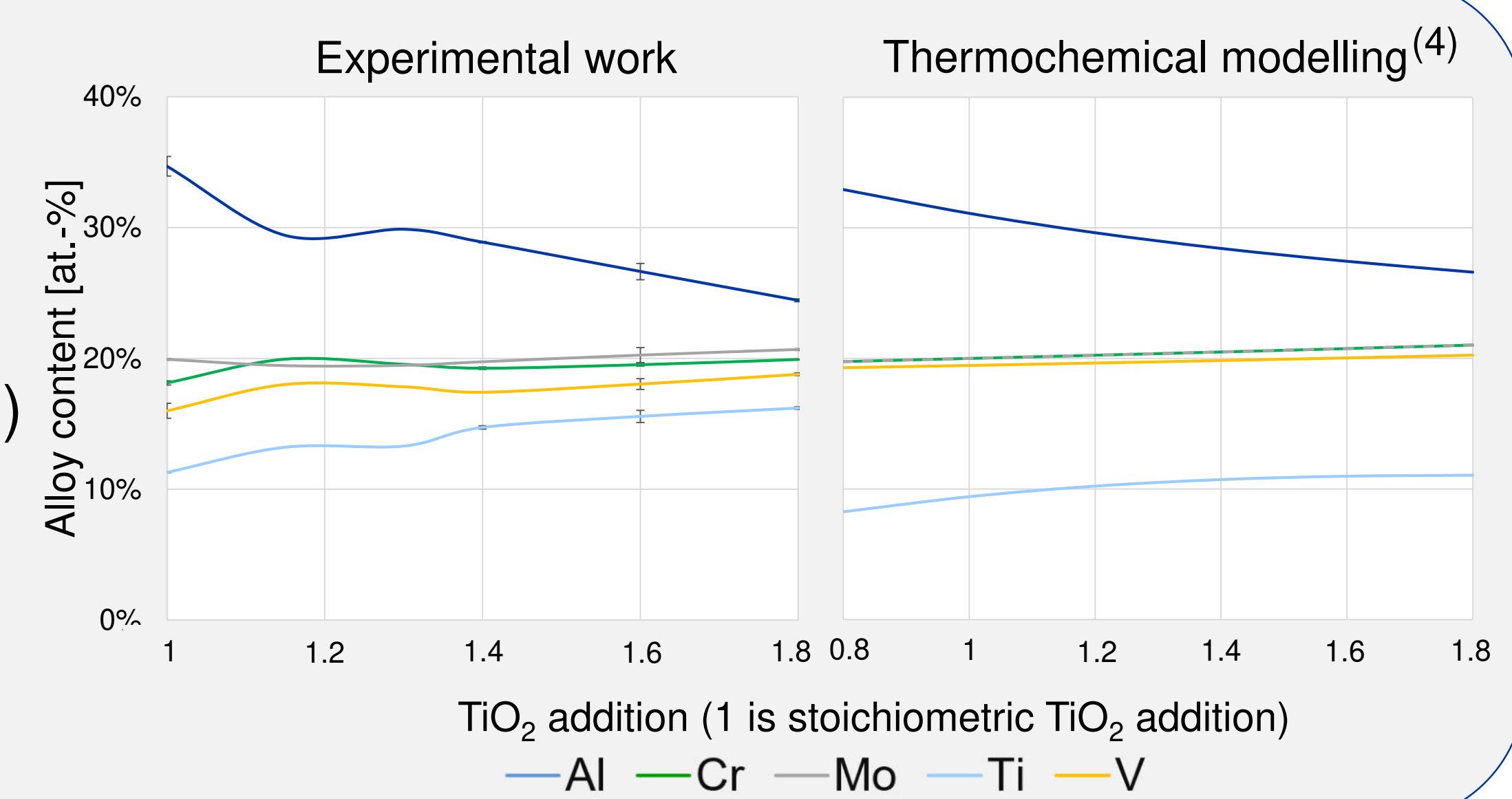
Production of multicomponent alloys through aluminothermic reduction possible

- Autothermal process with separation of metal and slag phase is given

### Comparison of thermochemistry and experiments

Generally good match between thermochemical modelling and experimental work:

- Reduction of refractory metal oxides good with conversion rates usually >80% (→ table 1)
- Ti conversion in trials better than thermochemically indicated
  - Positive effect that thermochemical equilibrium is not completely achieved
- Challenging issue is the reduction of TiO<sub>2</sub>
  - Insufficient conversion, Ti oxide remain in slag
  - Thus high proportion of unreacted Al in the metal phase



## Outlook

- Investigate reasons for insufficient TiO<sub>2</sub> reduction
- Why is the reduction inhibited and why do Ti oxides accumulate in slag
- Investigation of the mechanism of co-reduction of metal oxides
- Examine the influence of different metal oxides on the reduction of TiO<sub>2</sub>
- Phase analysis of the resulting metal product (e.g. REM-EDS)
- Examination of mechanical properties

## References

- Yeh, J.W. (2013): Alloy design strategies and future trends in high-entropy alloys. JOM 65: 1759-1771.
- Yeh, J.W., Chen, S.K., Lin, S.J., Gan, J.Y., Chin, T.S., Shun, T.T., Tsau, C.H., Chang, S.Y. (2004): Nanostructured high-entropy alloys with multiple principal elements: novel alloy design concepts and outcomes. Adv. Eng. Mater. 6, No. 5: 299-303.
- Gao, M.C., Yeh, J.W., Liaw, P.K., Zhang, Y. (2016): High-entropy alloys. Cham: Springer International Publishing. ISBN 978-3-319-27011-1.
- Bale, C.W.; Bélisle, E.; Chartrand, P.; Decterov, S.A.; Eriksson, G.; Gheribi, A.E.; Hack, K.; Jung, I.-H.; Kang, Y.-B.; Melançon, J.; et al. (2016): FactSage thermochemical software and databases. Calphad, 54, 35-53. ISSN 0364-5916.

Find more information here:



Carolyn Maier, M.Sc.  
IME – Institute for Process Metallurgy and Metal Recycling  
+49 240 80 95204  
cmaier@ime-aachen.de

**IME**  
DIE METALLURGEN

**RWTH AACHEN**  
UNIVERSITY



# **Model supported determination of the process window for aluminothermic synthesis of refractory high entropy alloys**

C. Maier\*, B. Friedrich\*

\* IME Institute for Process Metallurgy and Metal Recycling, RWTH Aachen University, Germany

## **Abstract**

Today's potential production methods for high entropy alloys show difficulties as they involve high-purity metals and reveal high energy consumption. In contrast, metallothermic reduction generally allow for decreasing production costs and time factors and thus overall efficiency by the use of exothermic enthalpy released during the reaction. Such, after successful proof-of-principle tests for equimolar high entropy alloys, this paper investigates the generation of binary to quintary alloys consisting of the elements Al, Cr, Mo, Ti and V as boundary systems.

To understand the complex reaction mechanisms of aluminothermic reduction of multicomponent alloys, thermochemical modelling is carried out using FactSage 8.0. Based on the outcome, the experimental parameters are derived allowing to reach the targeted alloy composition while simultaneously optimizing the input material mixture. Experimental validation takes place in 10 kg scale. Metal samples are analyzed via atomic emission spectroscopy, slag samples via X-ray fluorescence spectroscopy. As the fundamental work proves the concept the paper will also present results of the final alloy synthesis work.

## **Keywords**

Refractory high entropy alloys, metallothermy, SHS process, FactSage

## **Introduction**

In our everyday lives, the use of high-performance materials such as high-speed steels, superalloys or high-strength, lightweight Al alloys is well established. In the ongoing search for better and more efficient materials, high-entropy alloys, or short HEA, in particular are attracting increasing attention. These alloys are considered to be among the most promising candidates for meeting the ever-increasing demands placed on materials. In particular, materials used in plant construction for nuclear reactors, waste incineration plants and chemical plants or in turbine construction in the aerospace industry are constantly subjected to stresses close to their physical limits. Refractory high-entropy alloys (RHEA) made primarily from refractory metals designed to combine the advantages of high strength, high melting temperatures and low density with strong resistance to wear and oxidation. [1,2] However, the young alloy group is in development stage; so it is mainly produced on a laboratory scale. In future, production costs will have a

significant impact on the establishment of this alloy group in various applications. For this reason, the feasibility of producing HEA in an emission-free and cost-effective manner by using aluminothermy is being investigated.

The investigation of the process only by experimental methods is quite complex, expensive and time-consuming. Against the background of resource conservation, intensive thermochemical modelling of the alloy system leads to less required experiments. For this reason, predictions on the system are supposed to be made using the software FactSage [3]. In this way, conversion behavior of metal oxides, alloy compositions and limitations of the reduction system itself can be investigated.

The main goals of this work are (i) to investigate aluminothermic production of RHEA exemplified through AlCrMoTiV by thermochemical modelling in FactSage to obtain an optimal process window for aluminothermic synthesis, (ii) to show feasibility of the RHEA production through aluminothermic reduction and, finally, (iii) to evaluate the results of thermodynamic modelling by comparing them with corresponding results of experimental investigations.

### ***Refractory high entropy alloys***

There are two basic definitions of HEAs: The first definition refers to the composition of the alloys. According to this definition, HEAs are precisely those alloys that contain at least five and at most 13 major elements, with each major element contributing between 5 and 35 at.-% to the alloy. A minor element is defined as any added element contributing less than 5 at.-%. [5, 6, 7] The second definition leads to the name-giving high entropy [8, 9]. When alloying elements are added to an alloy, its configurational entropy increases; the more alloying elements are added, the greater the effect on this thermodynamic parameter. This results in the formation of a random solid solution and inhibits the creation of an intermetallic phase. As a result, alloys do not exhibit complex structures and, therefore, are not brittle but usable. [6, 10, 11]

RHEA represents a subgroup of HEA. These alloys consist primarily of refractory metals and show significant potential for the use in high-temperature applications [12]. Early research on RHEA investigated alloys with the refractory metals from Group V and VI (V, Nb, Ta and Cr, Mo, W) [12, 13]; later, elements of Group IV (Ti, Zr, Hf) were also added [14]. Ti was introduced to this composition because it is much lighter compared to the typical refractory metals. Despite improvement of the properties at room and elevated temperature alloys consisting only of refractory metals have a high density and low oxidation resistance. Therefore, in a next step, RHEAs were developed which also contain Al, which has a lower density than refractory metals and a positive effect on oxidation resistance.

### ***Aluminothermic reduction***

Metallothermic processes are based on the reduction of an oxide, chloride or fluoride metal compound by another, less noble metal, which has a higher affinity for oxygen or halides [15]. Characteristic feature of metallothermy is its autothermal process based on exothermic reactions and thus without external heat input, as well as the occurrence of high reaction temperatures of over 2500 °C [16]. As Fig. 1 shows, the heat dissipation in metallothermic reactions is prevented by the surface covered with molten feed, which keeps the heat loss by convection and thermal radiation at a minimum level. [16] Due to their thermochemical properties, alkali and alkaline-earth metals such as sodium, potassium, magnesium and

calcium, as well as aluminum, serve as reduction metals [15]. First, for a metallothermic reduction the dried metal compounds aimed to be reduced are mixed with the chosen reduction metal and charged into a reactor. Usually, both reactants are in the form of fine particles, for example as grit or chips. The reaction only takes place after the introduction of an activation energy, which is usually in form of an initial ignition. For this purpose, an ignition package is mainly used, which ignites the reaction mixture in its immediate surrounding by its released reaction enthalpy and thus initiates the reaction. [15, 16]

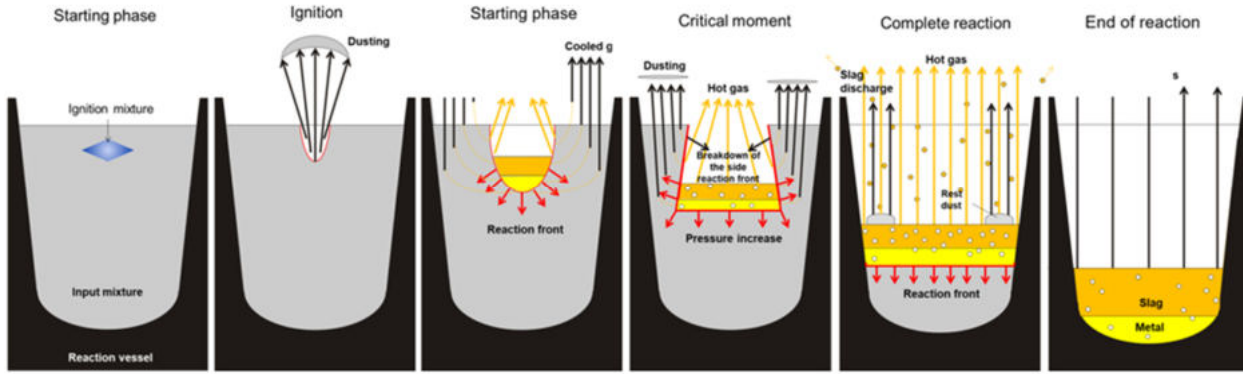


Figure 1: Procedure scheme for metallothermic reduction.

The stability of a metal compound can be approximated by the free enthalpy of formation (Gibbs energy)  $\Delta G_T^0$  [J], which results from the relationship between standard enthalpy of formation  $H_0$  [J], standard entropy of formation  $S_0$  [J K<sup>-1</sup>] and the temperature  $T$  [K] shown in equation (1). [16]

$$\Delta G_T^0 = \Delta H^0 - T \cdot \Delta S^0 \text{ bzw. } \Delta G_T^0 = -R \cdot T \cdot \ln p_{O_2} \quad (1)$$

A further possibility to define the free standard enthalpy of formation is depending on  $p_{O_2}$  the decomposition pressure of the oxide [Pa] and  $R$  the gas constant [J · mol<sup>-1</sup> · K<sup>-1</sup>]. The basis for the selection of a suitable reducing metal is feasible by comparing the thermodynamic properties of reactants and products. For this purpose, the formation of the respective reaction product is considered, depending on which metal compound is assumed (oxide, chloride or fluoride). In general, the reaction equation of a metallothermic reaction can be presented as follows [15, 16]:



where  $a$ ,  $b$ ,  $c$  and  $d$  represent stoichiometric coefficients,  $A$  the metal to be gained,  $B$  the reducing metal (in case of aluminothermic reduction the reducing metal is Al) and  $X$  either oxygen or halides.

Richardson-Jeffes diagrams can be a first step in considering whether reduction of the metal compound by the reducing metal will occur at the temperature considered. The diagram in Fig. 2 shows the standard free energy of formation released by selected metal-metal oxide reactions as a function of temperature. Reduction is possible when the free enthalpy of formation of the resulting metal compound (BX) is more negative than that of the starting metal compound (AX). [15] The diagram below shows that Al can act as a reducing metal for the other metal oxides being in focus of the present examination.

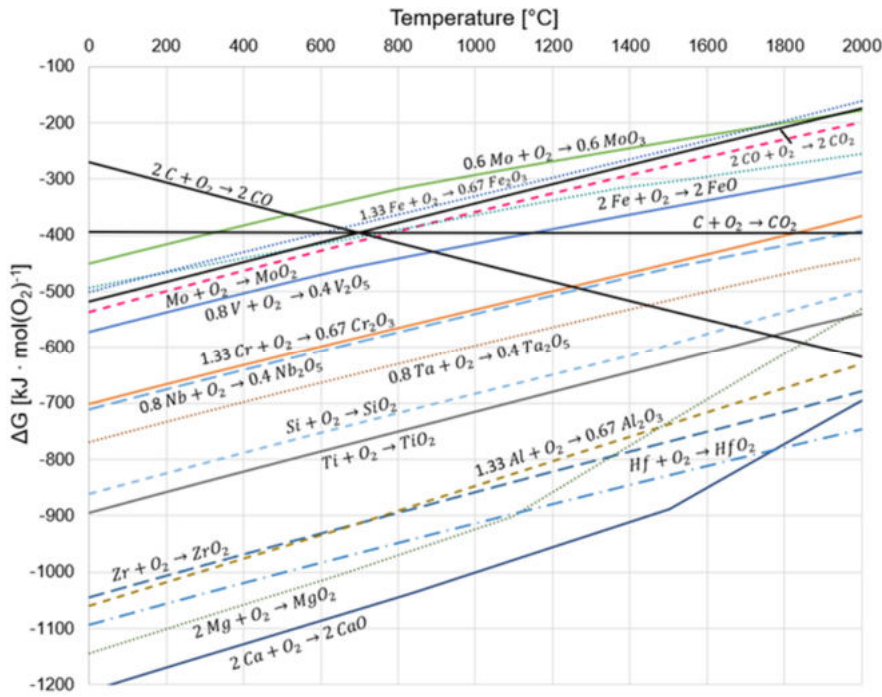


Figure 2: Richardson-Jeffes diagram for selected oxidation reactions. [3]

Based on known reaction enthalpies and empirical values, Shemtchushny has established a factor (SH factor) for the self-sustaining nature of metallothermic reactions. According to Shemtchushny, the amount of heat released must be  $2300 \text{ J} \cdot \text{g}(\text{input quantity})^{-1}$  [16]. This specific heat effect can be calculated by the following formula:

$$SH = \frac{\sum \Delta H_{298}^0}{m_{\text{input}}} \quad (3)$$

where SH the Shemtchushny factor,  $\sum \Delta H_{298}^0$  is the sum of the standard enthalpies of formation at  $25^\circ \text{C}$  [J],  $m_{\text{input}}$  is the total input mass [g].

Table I shows the reaction enthalpies and SH factors for the metal oxides used in this work for aluminothermic reduction.  $\text{TiO}_2$  reduction contributes the least energy to the aluminothermic process. However, with the help of other metal oxide reductions, sufficient energy is generated to maintain overall metallothermic process.

Table I: Reaction enthalpies of selected aluminothermic reductions according to FactSage [3].

Reaction	Reaction enthalpy [kJ/mol]	SH factor [J/g]
$0.75 \text{ TiO}_2 + \text{Al} \rightarrow 0.75 \text{ Ti} + 0.5 \text{ Al}_2\text{O}_3$	-129.3	-1189.1
$0.5 \text{ Cr}_2\text{O}_3 + \text{Al} \rightarrow \text{Cr} + 0.5 \text{ Al}_2\text{O}_3$	-274.3	-2197.4
$0.3 \text{ V}_2\text{O}_5 + \text{Al} \rightarrow 0.6 \text{ V} + 0.5 \text{ Al}_2\text{O}_3$	-372.7	-3604.5
$0.5 \text{ MoO}_3 + \text{Al} \rightarrow 0.5 \text{ Mo} + 0.5 \text{ Al}_2\text{O}_3$	-465.3	-3851.46

## Experimental

### *Methodology of thermochemical modelling with FactSage*

The Equilib module within FactSage 8.0 [3] works on the basis of Gibbs energy minimization. With this software, equilibrium states of reactions can be predicted after defining the input stream; thus gives a first indication of phases being expected in the experiments. As source the databases FactPS, FToxid and SGTE were used.

Figure 3 presents the alloys modelled and generated in experimental work. At this point, modelling is used to predict the composition of the resulting alloy. Initially, stoichiometric conversion of the metal oxides was assumed. Due to early recognition of the disfavored conversion of  $\text{TiO}_2$  when stoichiometric conversion was assumed, quantities added of both Al and  $\text{TiO}_2$  were varied as well as the energy density, which is adjusted by varying the amount of booster material  $\text{KClO}_4$ .

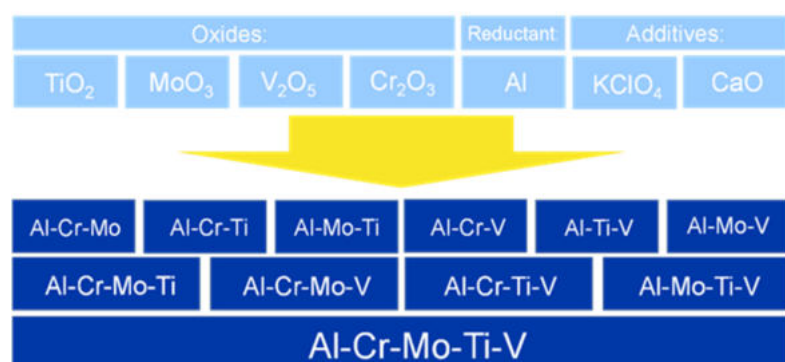


Figure 3: Alloys investigated by means of thermochemical modelling and experimental work.

### *Methodology of experiments*

The experimental part of the work aims to verify the possibility of RHEA production via aluminothermic reduction and to compare the products obtained with the results of the thermochemical modelling. Initially experiments were executed assuming stoichiometric conversion of the refractory metal oxides. Afterwards, experiments with additional  $\text{TiO}_2$  or a further variation of  $\text{TiO}_2/\text{Al}$  ratio are carried out. Examined parameters are based on the previously performed FactSage calculations. Fig. 4 depicts the metal oxide powders used in the aluminothermic reduction trials. In advance this feed material was dried at  $450^\circ\text{C}$  for 48 h to prevent humidity in the process. Fig. 5 shows the reducing metal Al,  $\text{KClO}_4$  acting as booster and the fluxing agent CaO.  $\text{KClO}_4$  was selected as booster material because of its thermal decomposition at process temperature and subsequent volatilization preventing any contamination of the final product. The KCl formed is transferred to the gas phase and extracted via an off-gas cleaning system. The addition of 30 wt.-% CaO to the calculated slag quantity improves slag properties with regards to decreasing liquidus temperature and viscosity supporting the separation of metal and slag.

Outcoming metal and slag product are mechanically removed from the reactor and separated from each other. Taken samples from both fractions are prepared separately in the further course by crushing, grinding and sieving. Chemical analysis is done by ICP-OES (metal) and XRF-WROXI (slag). Obtained results from first trials were the basis for optimization of feed material and thus specific adjustment of the desired alloy composition.

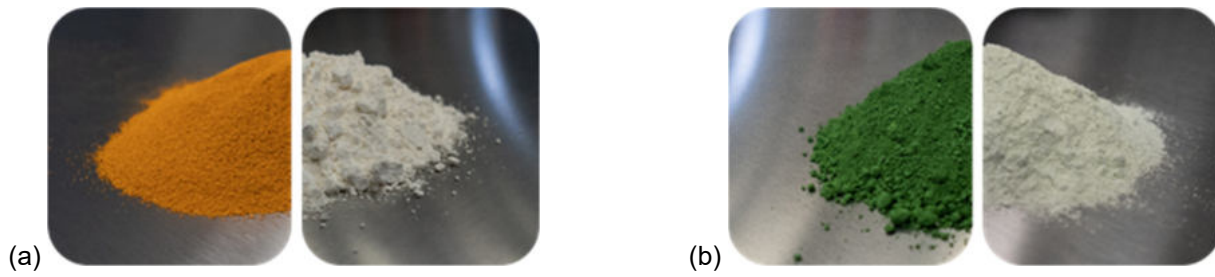


Figure 4: Metal oxides for ATR process: (a) V<sub>2</sub>O<sub>5</sub> (left) and TiO<sub>2</sub> (right), (b) Cr<sub>2</sub>O<sub>3</sub> (left) and MoO<sub>3</sub> (right).



Figure 5: Input materials for ATR process from left to right: Al as reductant, KClO<sub>4</sub> as booster and CaO as flux.

All experiments were carried out according to the same procedure. In the first step, all input materials were weighed and charged into a drum. This drum was placed in a drum hoop mixer to homogenize the feed material for 30 minutes. In the following, the homogenous mixture is charged into a corundum lined steel reactor. There, an ignition package consisting of KClO<sub>4</sub>, Mg chips and Al grit is placed on the surface of the feed material. The ignition is done electrically via resistance heating of a coil inside the ignition package. Table II presents the different input mixtures with the calculated SH factor at complete reaction. An illustration of the experimental procedure (on the example of the alloy AlCrMoTiV) can be seen in Fig. 6.

Table II: Input mixtures for trials conducted stoichiometrically

Alloy	Cr <sub>2</sub> O <sub>3</sub> [g]	MoO <sub>3</sub> [g]	TiO <sub>2</sub> [g]	V <sub>2</sub> O <sub>5</sub> [g]	Al [g]	CaO [g]	KClO <sub>4</sub> [g]	SH factor [J/g]
AlCrV	2926			3500	3830	2260	44	-2800
AlCrMo	2160	4114			3086	1874		-3061
AlCrTi	2996		3148		4278	2604	1410	-2800
AlTiV			3176	3616	4618	2872	632	-2800
AlMoTi		4214	2338		3502	2196	150	-2800
AlMoV		4140		2616	3622	2304		-3520
AlCrTiV	2138		2246	2558	4272	2846	922	-3000
AlCrMoV	1682	3187		2013	3386	2258		-3230
AlCrMoTi	1706	3230	1792		3498	2342	516	-3000
AlTiMoV		3248	1802	2052	3690	2496	74	-3000
AlCrTiMoV	1390	2630	1460	1662	3574	2494	236	-3000



Figure 6: Illustration of the aluminothermic reduction of AlCrMoTiV.

## Results and discussion

### *FactSage calculations (with FactSage)*

In order to obtain an overall view on the reduction experiments for the production of the quintary equimolar alloy AlCrMoTiV, the ternary and quaternary alloy sub-systems were first investigated under stoichiometric Al addition. In this context it was found that the alloy systems consisting of Cr, Mo and V in combination with Al yielded good results. An almost 100 % conversion of the oxides have been achieved. When  $\text{TiO}_2$  was added to the feed mixture in thermochemical modelling, the good conversion rates of the other refractory metal oxides could still be demonstrated. However, the overall metal yields have decreased which is due to the fact that  $\text{TiO}_2$  was insufficiently reduced. Table III shows the conversion rates of  $\text{TiO}_2$  in the various input mixtures at stoichiometric addition of Al. It can be seen that the reduction of  $\text{TiO}_2$  occurs to a lower extent than for the other refractory metal oxides. In addition, the Ti conversion rate decreases as the number of alloying elements is increased. In the modelling results, the worst conversion with 47.18 % is to be expected in the five compound system. Further correlation can be observed for co-reduction of  $\text{Cr}_2\text{O}_3$  as it indicates a disruptive effect on  $\text{TiO}_2$  reduction.

Table III: Thermochemical modelled conversion rates of Ti for selected alloy systems [3]

Alloy	Ti conversion rate [%]
AlCrTi	64.12
AlMoTi	75.35
AlTiV	65.03
AlCrTiV	49.74
AlCrMoTi	58.09
AlMoTiV	60.60
AlCrMoTiV	47.18



An approach to enhance the before mentioned poor conversion rates was made by determining if the addition of further  $\text{TiO}_2$  to the feed mixture will have a positive effect on the targeted alloy composition. At this point it was assumed that a saturation of the Ti oxide concentration in the slag occurs, accompanied by an increased activity of this component in the slag. Thus, the reduction of  $\text{TiO}_2$  will be supported. Thermochemical modelling confirmed this assumption and, moreover, stressed out that excessive Al content in the final alloy needs to be adjusted by reducing its input. This relationship is visualized in Fig. 7. Both, increasing  $\text{TiO}_2$  content and lowering Al input mass in the feed material leads to a more even distribution of all alloying components getting closer to aimed equimolar composition. With regard to the slag phase, the enrichment of refractory metal oxides in the slag only takes place to a low extent for Cr oxides; the oxides of Mo and V scarcely accumulate in the slag. This suggests that the reaction equilibrium of the metal oxide reduction is mainly on the product side.

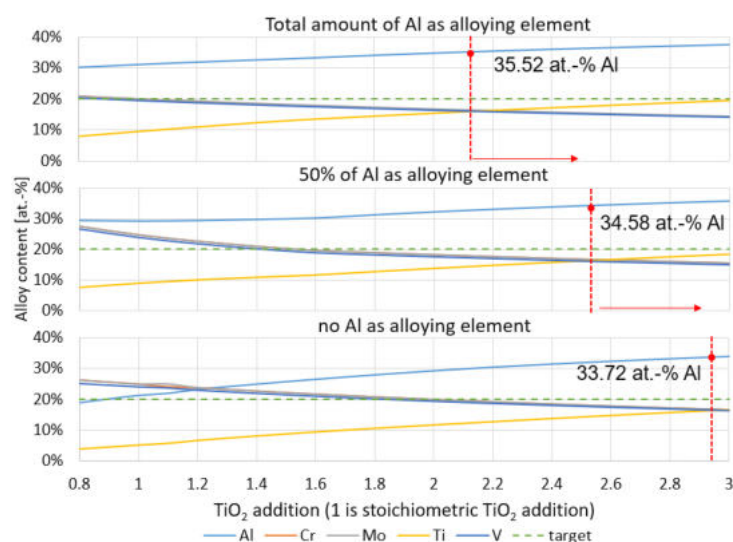


Figure 7: Influence of Al mass input on alloy composition according to FactSage [3].

Furthermore, the influence of the energy density on the reduction of metal oxides was investigated. Here it is assumed that increasing energy density is accompanied by a rising temperature, which in turn leads to improved metal/slag separation. In practice, however, it appears that increasing energy density also results in stronger splashing and higher amount of waste gas due to the decomposition of the booster material  $\text{KClO}_4$ .

To investigate the influence of energy density, the input mixtures with stoichiometric Al addition were tested at different SH factors. Here,  $-3000 \text{ J} \cdot \text{g}^{-1}$ ,  $-3200 \text{ J} \cdot \text{g}^{-1}$ ,  $-3400 \text{ J} \cdot \text{g}^{-1}$  and  $-3600 \text{ J} \cdot \text{g}^{-1}$  were chosen to examine the impact on metal concentration for Al, Cr, Mo, Ti and V in the final alloy. The alloy composition changes only marginally due to increasing energy density in the system. The amount of extracted metal phase, on the contrary, decreases minimally by 14.3 g in average when increasing SH factor by  $200 \text{ J} \cdot \text{g}^{-1}$ . In conclusion, the energy density has a marginal effect on the alloy composition. This can be explained by the fact that in FactSage modelling only thermochemical equilibria are considered neglecting the influence of kinetics. Thus, in the present case, the reduction of the refractory metal oxides takes place the same way.

## Experimental results

After experimental procedure of the aluminothermic reduction metal and slag phase remain as product. A visual assessment of both products reveals homogeneous surface conditions as presented in Fig. 8 (a) and (b). Subsequent to easy separation of metal and slag and crushing of the brittle metal product a uniform structure without any segregation becomes obvious in Fig. 8 (c) by the example of AlCrMoTiV alloy.

Slags produced in the various trials presented different surface stains. Thus, slags containing V oxides were more yellowish/orange in color, whereas slags containing Mo oxides appear in brown color. Slags containing Cr oxides showed a greenish shade. Despite low concentrations of these refractory metal oxides in the slag, the appropriate change in color on the slag surface can be traced to direct contact with the atmosphere at high reaction temperature; here it can be assumed that the oxides reach their highest possible oxidation state resulting in coloring the surface of the slag in their specific colors. After crushing the slag, it showed a grey color with cavities caused by escaping gas during the solidification of molten slag.



Figure 8: (a) Slag surface, (b) metal surface and (c) metal product of AlCrMoTiV.

After completion of the experimental part, analysis of the generated metal and slag samples were performed. The evaluation and assessment of the analysis results is presented in the following.

Table IV summarize the average conversion rates of the various alloying elements in different alloys. At this point it becomes evident that high conversion rates can be obtained in the absence of Ti in the target alloy. This changes when  $\text{TiO}_2$  is added to the input mixture as the metal yield is lowered due to the poor reduction of  $\text{TiO}_2$ . However, all other refractory metals have conversion rates above 80 % when excluding Ti in the alloy system, with the exception of V in the quaternary and quintary alloys.

The correlation that an increasing number of alloying elements adversely affect the conversion rate for  $\text{TiO}_2$  was also found in the previous chapter about thermochemical modelling. Thus, the conversion rates in ternary systems are on average 57.6 % (when neglecting worst conversion rate of 44.2 % for AlCrTi the average is 64.4 %), in quaternary systems the average value is 60.3 %, and in quintary systems the mean is 51.2 % in case of stoichiometric addition of Al. Compared to the thermochemical modelling, even higher conversion rates have been obtained for  $\text{TiO}_2$ , which is reflected in a higher Ti concentration in the aimed alloys. This suggests that the system is not yet in thermochemical equilibrium when the metal and slag are solidified. Once falling below liquidus temperature, the alloy freezes and accordingly other compositions compared to thermochemical modelling may be formed.



Table IV: Mean values of the conversion rates shown for selected trials

Conversion rates	Cr [%]	Mo [%]	Ti [%]	V [%]
AlCrMo	83.7	89.1		
AlCrTi	69.3		44.2	
AlCrV	89.7			82.1
AlMoTi		87.8	58.6	
AlMoV		95.3		84.7
AlTiV			70.1	92.6
AlCrMoTi	81.1	89.5	58.7	
AlCrMoV	86.0	91.3		83.0
AlCrTiV	92.8		70.4	89.6
AlMoTiV		87.1	51.8	77.3
AlCrMoTiV	82.2	90.4	51.2	72.6
AlCrMoTiV (more TiO <sub>2</sub> )	88.1	91.2	69.8	81.5

The achievement of the targeted chemical composition for various alloys was also closely examined. As an example, the alloy AlCrMoTiV generated at a stoichiometric addition of Al is presented in Fig. 9. It illustrates a direct comparison between the thermochemically calculated composition and the product of experimental work. First of all, it can be stated that both show similar tendencies: TiO<sub>2</sub> cannot be completely reduced, which results in an increased Al content in the alloy. The diagram also points out that the Ti concentration is slightly higher in the experimental part of the work by contrast with thermochemical modelling. This in turn can be explained by the solidification of the resulting metal phase initiated before thermochemical equilibrium is reached. Similar correlations were found as well for the other alloys.

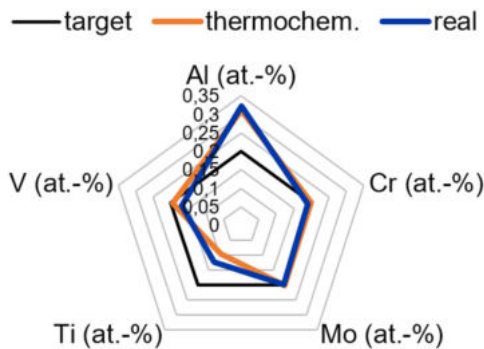


Figure 9: Target, thermochemical and product (real) composition of stoichiometric AlCrMoTiV trials.

Furthermore, a closer look at the overstoichiometric TiO<sub>2</sub> addition was also taken in terms of experimental investigation. The overstoichiometric addition of TiO<sub>2</sub> allows higher conversion rates, being 69.8 % on average, for this component than compared to stoichiometric addition of TiO<sub>2</sub>. As illustrated in Fig. 10, experimental validation of thermochemical modelling is successfully carried out. Similar behavior

can be seen for the alloy composition: by raising the amount of added  $\text{TiO}_2$ , the initial objective of reaching an equimolar composition can be achieved. At the same time, rising concentration of Ti oxides in the slag was also observed with overstoichiometric  $\text{TiO}_2$  addition. For this reason, it is obvious that increasing  $\text{TiO}_2$  concentration in the slag actually leads to an increase in  $\text{TiO}_2$  activity and thus enhances the reduction.

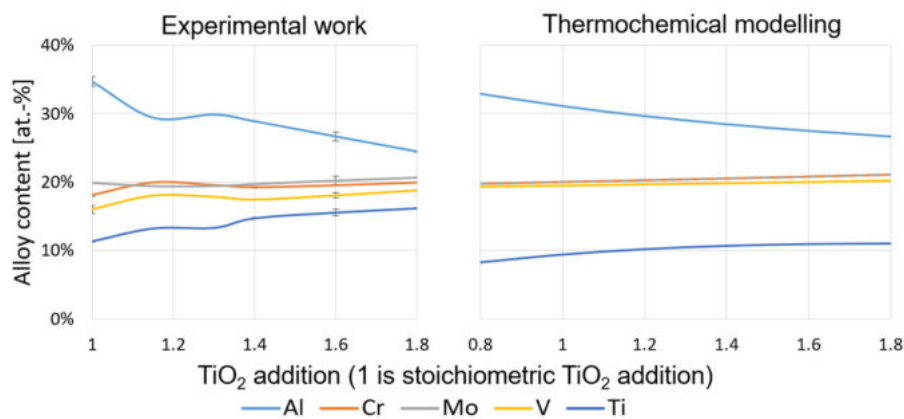


Figure 10: Results of experimental work and thermochemical modelling on overstoichiometric  $\text{TiO}_2$  addition [3].

## Summary and Outlook

With regard to new production technologies, new opportunities are emerging in the field of RHEA production. The present work shows that the production of equimolar multicomponent alloys with five components is possible by means of aluminothermic reduction. This was demonstrated in both the thermochemical modelling and the experimental part of this work.

By using the thermochemical software FactSage, the five compound system is first investigated in detail with regard to the resulting phases. Adjustment of the input material mixture offers the possibility to generate findings depending on various influencing factors (and therefore to optimize the examined process). It became apparent at an early stage that the conversion of  $\text{TiO}_2$  to metallic Ti do not proceed to a sufficient degree. By adding additional  $\text{TiO}_2$  to the input mixture, the Ti content in the final alloy have been increased to an intended level. Moreover, a decreasing amount of added aluminium shows a suppressing effect on  $\text{TiO}_2$  conversion. This circumstance can be explained by preferred conversion of the more noble refractory metal oxides, so that additionally added  $\text{TiO}_2$  remains in the slag for lack of reducing agent.

These outcomes from thermochemical modelling were confirmed in experimental work. Precise adjustment of the aimed composition can be achieved without problems in case of absence of Ti. Adding Ti as a further component to the alloy system diminish the overall metal yield due to insufficient reduction of  $\text{TiO}_2$ . Against this background unreacted Al remains in the metal phase, which is leading to both reduced Ti and elevated Al content in the product. By adding supplementary  $\text{TiO}_2$  to the input mixture, the composition of the alloy has been improved in view of equal distribution of all alloying elements. Here, it must be considered whether this procedure is economically feasible due to additional costs for  $\text{TiO}_2$  being slagged in the course of aluminothermic reduction.



Thus, in future experiments it is foreseen to test the addition of Ti sponge as a remedy for unsatisfactory Ti concentration in the resulting alloy. For this purpose, Ti sponge is going to be put on the bottom of the reactor, on which the remaining input mixture will be placed. Due to the high reaction temperatures during aluminothermic reduction and settling down of the metal phase to the bottom of the reactor, Ti sponge will melt and merged into the resulting metal phase.

Furthermore, for the specific adjustment of phases as well as a directional solidification, the most promising experiments will be carried out in a water-cooled copper mold. Some investigations are still necessary to go this step, such as the exact implementation of the energy density because of higher heat extraction in the water-cooled mold. A possible utilization of additional Ti sponge, for the reason described above, needs also to be proved in the water-cooled reactor concerning its melting behaviour in a cooled environment.

## References

- [1] R. Steiner, ASM Handbook Volume 1: Properties and Selection: Irons, Steels, and High-Performance Alloys, ASM International, (1990)
- [2] R. Steiner, ASM Handbook Volume 2: Properties and Selection: Nonferrous Alloys and Special-Purpose Materials, ASM International, (1990)
- [3] C. W. Bale, E. Bélisle, P. Chartrand, S. A. Decterov, G. Eriksson, A.E. Gheribi, K. Hack, I. H. Jung, Y. B. Kang, J. Melançon, A. D. Pelton, S. Petersen, C. Robelin, J. Sangster, P. Spencer and M-A. Van Ende, *Calphad* Vol. 55, 1-19, (2016)
- [4] M. C. Gao, J.-W. Yeh, P. K. Liaw und Y. Zhang, *High-Entropy Alloys*, Springer, Cham, (2016)
- [5] J. Yeh, S. Chen, S. Lin, J. Gan, T. Chin, T. Shun, C. Tsai und S. Chang, *Adv. Eng. Mater.* Vol. 6, 299-303, (2004)
- [6] J.-W. Yeh, *JOM* Vol. 65, 1759-1771, (2013)
- [7] D. Miracle, J. Miller, O. Senkov, C. Woodward, M. Uchic, J. Tiley, *Entropy* Vol. 16, 494-525, (2013)
- [8] B. Murty, J.-W. Yeh, S. Ranganathan, *High-Entropy Alloys*, Elsevier, Amsterdam, (2014)
- [9] F. Otto, Y. Yang, H. Bei, E. George, *Acta Mater.* Vol. 61, 2628-2638, (2013)
- [10] B. Cantor, *Ann. Chim. Sci. Mat.* Vol. 32, 245-256, (2007)
- [11] K. Tsai, M. Tsai und J. Ye, *Acta Mater.* Vol. 61, 4887-4897, (2013)
- [12] O.N. Senkov, G.B. Wilks, D.B. Miracle, C.P. Chuang, P.K. Liaw, *Intermetallics* Vol. 18, 1758-1765, (2010)
- [13] O.N. Senkov, G.B. Wilks, J.M. Scott, D.B. Miracle, *Intermetallics* Vol. 19, 698-706, (2011)
- [14] O.N. Senkov, D.B. Miracle, K.J. Chaput, J.-P. Couzinie, *J. Mater. Res.* Vol. 33, 3092-3128, (2018)
- [15] R. Kieffer, G. Jangg, P. Ettmayer, *Sondermetalle*, pp. 27-147, Springer, Wien, (1971)
- [16] W. Dautzenberg, *Ullmanns Encyklopädie der technischen Chemie*, pp. 351 - 361, Bartholome, Weinheim/Bergstraße, (1974)